Jestr

Journal of Engineering Science and Technology Review 15 (5) (2022) 204 - 209

JOURNAL OF
Engineering Science and Technology Review

Review Article

www.jestr.org

Recent Progress of Tapered Optical Fiber for Biosensing Applications

Thanigai Anbalagan[1], Hazura Haroon[1,*], Huda Adnan Zain[2], Hazli Rafis[1] and S.W. Harun[2]

[1]*Center for Telecommunication Research and Innovation, Faculty of Electronic and Computer Engineering, Universiti Teknikal Malaysia Melaka, Hang Tuah Jaya, 76100 Durian Tunggal Melaka, Malaysia*

[2]*Department of Electrical Engineering, University of Malaya, Kuala Lumpur 50603, Malaysia*

Received 19 August 2022; Accepted 28 August 2022

Abstract

The development of reliable, lightweight, and effective sensors is a vital step in effectively monitoring critical parameter changes. This review focuses on the utilization of tapered optical fiber as a material sensing platform. The fundamental concept of the tapered fiber sensor is based on the interaction of strong evanescent waves caused by the fiber's dimensional change. The primary goal of this review is to explore the potential of tapered optical fiber for biosensing applications. A number of tapered optical fiber configurations and operations have been reviewed in order to propose appropriate optical sensor designs for biosensing applications. Hence, this analysis could serve as a benchmark for a more thorough study of biosensing device development.

Keywords: Tapered Fiber, Biosensor, Fiber Sensor, Biomedical, Fiber Applications

1. Introduction

This paper explores the most recent applications and achievements of optical fiber sensors (OFS) and technology in biosensing applications. The first section of this paper introduces various optical fiber configurations, such as tapered fiber, cladding-removed fiber, interferometers, and fiber grating. The applications of these tapered fiber sensors in biosensing applications are then discussed with a focus on glucose, pathogen, and protein sensing.

Optical fiber sensing has been developed as a cost-effective and versatile technology that can be utilized in various applications. Research on OFS began in the 1960s, but the technology was not fully utilized until the 1980s, when improved low-loss fiber optics enabled the technology to progress from the experimental stage to practical applications [1]. Several early low-loss optical fiber sensing studies were conducted in the early 1970s [2, 3].

Various benefits of using OFS include small bulk, lightweight, anti-electromagnetic interference, long-distance transmission, and in situ monitoring, and these benefits have sparked much interest in the monitoring of parameter changes. As a result, OFS are widely used in a variety of fields to measure parameters, such as strain, temperature, vibration, and displacement [4-6]. Researchers are intrigued by OFS due to their safety, pollution-free operation, corrosion resistance, remote sensing capability, anti-electromagnetic interference, and other remarkable properties. Physical, chemical, and biological measurands can communicate with light directed by an optical fiber to generate a modulated optical signal containing measurement parameter information [7].

An optical fiber can be single-mode or multimode depending on the core size, operating wavelength, and refractive index (RI) difference. The most common type of fiber is single-mode fiber (SMF). This type of fiber is typically composed of three layers: silica core, silica cladding, and buffer coating. The silica core is usually 2–10 μm, and it can be doped with nanomaterials to increase its RI. The size of the cladding is typically 125 μm in diameter. The buffer coating has no effect on light propagation; instead, it protects and strengthens the fiber. Plastic [8] is another material that can be used to make optical fibers. For biosensing, OFS detect changes in light propagation caused by external stimuli ranging from physical (e.g., stress) to biological (e.g., analyte concentration and chemical composition) components [9]. This is a one-of-a-kind feature because it enables the identification of specific biological traits or profiles that can be mapped to optical profiles [10]. The following subsections discuss different types of fiber configurations, such as tapered fiber, cladding-removed OFS, interferometers, and grating-based OFS.

1.1 Cladding-Removed OFS

Cladding removal is the simplest way to achieve direct interaction of light with the medium surrounding the optical fiber. Figure 1 shows the illustration of OFS with removed cladding. In certain applications, the degree of evanescent wave (EW) penetration into the low-index medium must be regulated. This quantity is often characterized by the penetration depth, d_p. The magnitude of the penetration depth can be described by:

$$d_p = \frac{\lambda}{2\pi n_1 \left[\sin^2\theta - \left(n_2 / n_1^2 \right) \right]^{1/2}} \quad (1)$$

Where λ is the vacuum wavelength, θ is the angle of incidence to the normal at the interface, and n_1 and n_2 are the refractive indices of the dense and rare media, respectively [11]. Cladding removal is well-known for plastic optical fiber (POF) and multimode fiber (MMF) [12, 13, 14]. Cladding-removed plastic fiber has high reproducibility and low

*E-mail address: hazura@utem.edu.my
ISSN: 1791-2377
doi:10.25103/jestr.155.25

fabrication costs, making it suitable for fiber optic sensing applications. The MMFs outperform POFs in terms of loss and can be coupled to other SMF telecom segments, making them suitable for remote sensing applications [15].

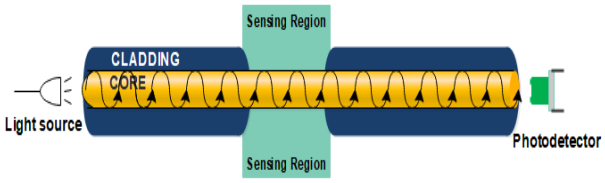

Fig. 1. Illustration of OFS with removed cladding.

There are several variations of cladding-removed OFS, such as D-shape [16, 17], U-shape [18, 19], and modified cladding [20]. D-shape removed cladding has several advantages, including a high potential for real-time monitoring in analytical chemistry and industrial applications, as well as also ease of fabrication. [17]. U-shaped sensors stand out for their high sensitivity and ease of use because these sensors can be dipped directly into the sample [19]. In clad-modified OFS, light propagating through the fiber is intentionally leaked for sensing purposes. Figure 2 shows the illustration of two types of OFS.

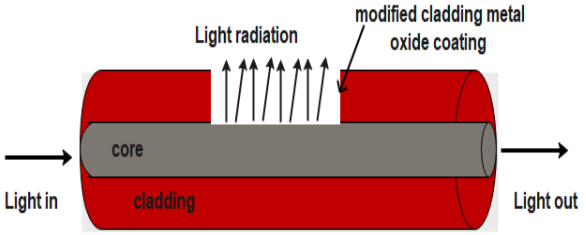

a)

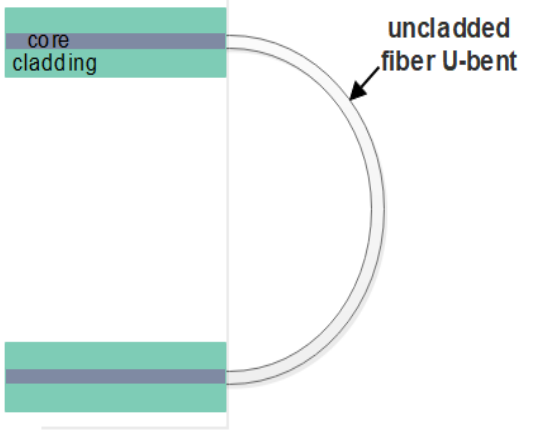

b)

Fig. 2. Illustration of OFS (a) modified partially cladding removal OFS (b) U-shape OFS

1.1.2 Basic Experimental Setup for Tapering

Using a relatively short section of optical fiber is one of the simplest methods for making fiber optic sensor elements (with lengths ranging from sub-millimeter to tens of millimeters) [21]. This allows access to the EW modes, which propagate in the tapered zone and allow contact with the medium for parameters, such as RI measurements. The focus of this review is to explore the potential of tapered optical fiber for sensing purposes. An OFS can be tapered using chemical etching, as shown in Figure 3. In Figure 3(a), standard multimode SK-80 POF fiber was used for tapering. Fluorinated polymer jackets with a diameter of 1,880–2,120 nm were used as the POF's outer layer. First, the POF's jacket was stripped to the desired length, as depicted in Figure 3(b). The fiber was tapered using acetone, deionized water, and sandpaper (Figure 3(c)). The POF's sensing region was then exposed to an acetone solution using a cotton bud. Around the POF's outer cladding, exposure to acetone resulted in a milky white surface. The sensing area and cladding portion were stripped and removed with sandpaper until the initial waist diameter of the tapered POF was reached.

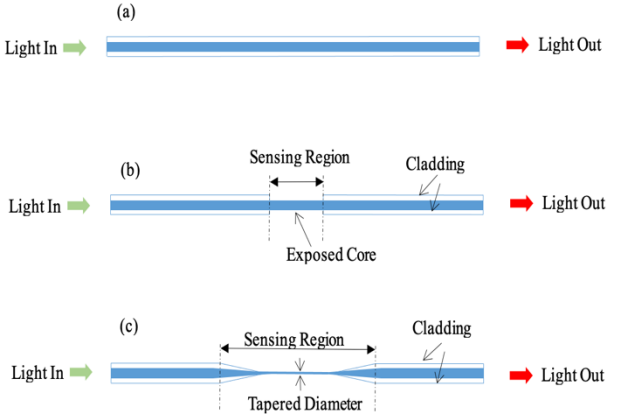

Fig. 3. POF tapering using chemical etching

Presuming that the directed field can penetrate deeply enough, it is necessary to remove most of the sheathing to achieve high sensitivity. The ability of the probe to internally reflect light would be disrupted if the core-cladding interface depleted during removal; therefore, caution should be exercised to avoid this conduction. As a result, the cladding should be carefully stripped off until only a thin layer is left. Furthermore, the core-cladding interface needs to remain largely intact.

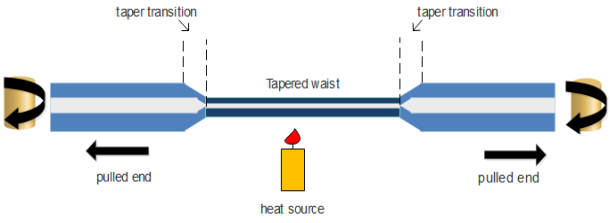

Fig. 4. Schematic illustration of the flame approach used for the fabrication of tapered OFS

1.2 Tapered Fiber

In addition to chemical etching, optical fiber can also be tapered by heating a fiber part and pulling the ends of the fiber together, as shown in Figure 4. Each tapered fiber reflection output spectrum is determined by its conical section profile, waist diameter, and the reflectance index of the surrounding medium. The power in the EW and the interaction with the surrounding medium increase as the taper tail diameter decreases and the RI difference between the fiber and the surrounding medium decreases [22, 23].

Tapered optical fibers are classified as adiabatic and non-adiabatic. The angle of the taper transition region is small (10^{-4}–10^{-3} rad) in adiabatic configuration, and the cylindrical symmetry of the optical fiber is preserved (with a taper ratio of taper diameter to initial diameter of the core (a/a0) between 0.2 and 1), resulting in the majority of the optical power

remains in the fundamental mode [24]. A taper is adiabatic if the angle of the taper is sufficient to reduce the power of the fundamental mode throughout the taper. The linear polarized fiber mode is generally combined with hybrid, HE_{11}, and HE_{12}. Non-adiabatic tapers have diameters of no less than 10 µm [25]. Some light with the basic mode connects to the high-quality cladding mode as it propagates to the taper. Due to a significant reduction in the diameter of the uniform tapering waist, much of the evanescent field of the tapered fiber is spread into the external environment [26].

Tapered fiber sensors have many applications, including sensing gas [27, 28], biomolecules [26, 29], and chemical molecules [30]. The tapered fiber sensor is attractive for in situ, real-time protein, toxins, DNA, and bacteria-monitoring applications. The mechanism and applications of tapered OFS for biosensing applications are discussed in Section 2.

1.3 Fiber Bragg Gratings

Fiber Bragg gratings (FBG) are a common and well-established technology in biosensing fiber optic sensors. The structure of FBG has lower insertion losses and a spectral transfer function that is easily tailored. Furthermore, this structure can be mass-produced at low costs [31]. A fiber grating structure has a segment with periodic perturbations (Λ) of the RI of the rest of the core. Moreover, FBG can be classified based on the period of these perturbations. Short-period FBG are perturbations with a period in the hundreds of nanometers, while long-period gratings are those with a period of between 100 and 700 µm [32–35].

The coupling between the forward propagating mode and the counter-propagating mode inside the fiber is the basis for the operation of FBG sensors. The average effective RI of the core mode is n_{effcor} [33, 35]. Both n_{effcor} and Λ are affected by temperature and grating variations. Typically, FBG sensors are based on the phenomenon of resonance wavelength shift caused by these temperature changes, grating tension, or grating compression. An example of an FBG sensor and its output spectra is shown in Figure 5 [33]. If a broadband light spectrum is launched into the FBG sensor, the FBG reflect the resonance wavelength, and the rest of the input spectrum passes through the gratings. It is possible to record and examine the reflected spectrum using couplers or circulators. As the resonant wavelength depends on the RI of the perturbations, FBG are sensitive to changes in the environment. As a result, the resonance wavelength changes as the environment around it does and using FBG structures as sensors involves tracking these resonance wavelength changes [32]. Some FBG variability has been proposed to improve FBG sensitivity to the RI. Tilted FBG have periodic perpetuation at an angle of less than 10° to the main fiber axis. This structure has a similar wavelength resonance to regular FBG. Furthermore, several cladding modes are excited at the cladding and outer medium boundaries. If the fiber is coated with an end reflector, the reflections of these modes appear as a comb of narrow wavelength for $\lambda < \lambda_{res}^{FBG}$ [34, 36, 37].

Reports have been documented earlier that FBG have been used to sense relative humidity changes, strain, temperature, magnetic field, and electric current [38-41]. Due to their sensitivity to strain and temperature changes, FBG are also useful for biosensing applications. FBG sensors, for example, have been used to detect diabetic patients' foot pressure [42]. However, FBG sensors face several challenges, including temperature and strain cross-sensitivity, a lack of standardized data interpretation technology, and the need for high-resolution devices to detect wavelength shifts and spectra [32].

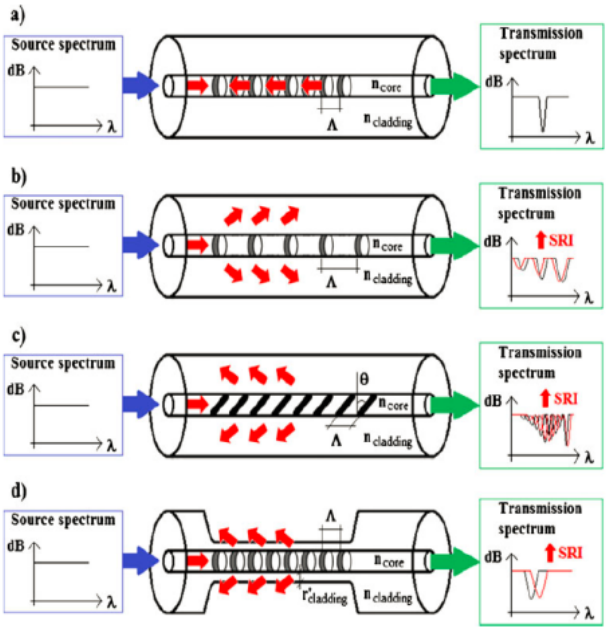

Fig. 5. FBG structure and their corresponding output [33]

1.4 Interferometers

An interferometer fiber sensor has inspired the interest of many researchers due to its ultra-compact structure and ability to perform a wide range of sensing functions. It has been used to measure the RI, vibration, micro-displacement, and other parameters [43]. Optical interferometers are also used in optical modulation, signal processing, and also physical, chemical, and biological sensing applications [44].

Fiber optic interferometers are based on the interference of higher-order and fundamental modes, resulting in a sinusoidal channeled transmission spectrum with fringes. According to [45], the phase of the spectrum's fringes is determined by the difference in optical path lengths of the interfering modes.

$$\delta_{FPI} = \frac{2\pi}{\lambda}(\delta n_{eff})L \tag{2}$$

Where λ is the wavelength, L represents the distance between two coupling elements, and δ_{neff} denotes the difference in refractive indices between higher-order and fundamental modes.

Fiber optic interferometers include the Fabry-Perot [45], Mach-Zehnder [46], Michelson (MI) [47], and Sagnac [48] configurations, each of which has a representative performance. The operating principles and fabrication techniques differ for each type of sensor. Fabry-Perot interferometers consist of two parallel reflecting surfaces that are separated by a predetermined distance. There are numerous uses for Mach-Zehnder interferometers (MZIs) owing to their versatility. Figure 6 shows a schematic illustration of an optical fiber modal MZI [49].

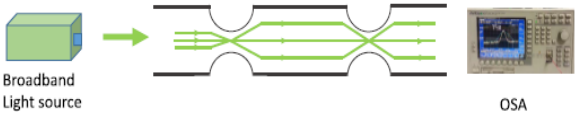

Fig, 6. Schematic illustration of an optical fiber modal Mach-Zehnder interferometer

There is not much difference between MZIs and MI-based fiber optic sensors. In an MI, two arms of light interfere with one another, but the ends of each arm reflect one of the reflected beams. Sagnac interferometers (SIs) have recently gained popularity in a wide range of sensing applications due to their advantages in terms of simple structure, ease of production, and environmental robustness, making them ideal for field testing and large-scale production [50-51].

2. Tapered OFS Application in Biosensing Systems

The implementation of tapered optical fibers has been observed in the development of numerous recent biosensing systems. Among them are enzyme detection, pathogen and pesticide detection, glucose level measurement, and protein detection.

2.1. Enzyme Detection

Enzymes are proteins that catalyze biological and chemical reactions. Enzymes function in three different ways. The enzyme first converts the sample into a detectable product. Second, the sample either inhibits or activates the enzyme, causing a signal to be translated. Finally, a signal is generated based on the changes made to the active site of the enzyme after the sample has been bound [52-54].

This subtopic discusses enzyme-based biosensors. For optical fiber biosensors, the immobilization matrix serves as a domain. This is done to maintain the stability and sensitivity of the detected enzyme. An optical fiber biosensor was developed in [55] to primarily detect uric acid. Two probes were fabricated, one with graphene oxide and the other with gold nanoparticles.

As reported by [56], a tapered fiber optic biosensor was developed to detect the taurine enzyme. The taurine dioxygenase enzyme was immobilized on a gold nanoparticle coating that encapsulated the sensing region. In this study, the sensitivity of the probe was shown to decrease with increasing taurine concentration. The maximal sensitivity value increased by 0.0190 AU/mM as the taurine concentration decreased to zero. This sensing probe's advantages include compactness and low fabrication costs.

The evanescent field method was used in [57, 58] to detect enzymes. In [58], a novel method for detecting triacylglycerides was reported by immobilizing zeolitic imidazolate framework-8 (ZIF-8) packaged lipase on a tapered fiber sensing region. To alter the sensitivity of the enzyme, the tapered fiber diameters were varied. The sensor probe with a diameter of 7 μm of fiber-tapered region had the highest sensitivity of 0.9 nm/nM. In another study, [57] developed a tapered fiber sensor coated with polyaniline-zinc oxide (PANI-ZnO) and immobilized with urease over the sensing region. This sensing probe demonstrated high sensitivity and stability, with a detection limit of 10 nM for urea concentration. The key performance of the tapered optical fiber that has been discussed is summarized in Table 1.

Table 1. Comparison of tapered optical fiber results in enzyme application

Sensing Structure	Sensitive Film	Mechanism Used	Sensitivity	Linear Range	Detection Limit	Ref
Tapered Based Sensor	Gold Nanoparticles/ taurine Dioxygenase	LSPR	0.0190 AU/mM	0 to 1 mM	53 μM	[56]
	Graphene Oxide / Uricase	LSPR	0.0089 nm/μM	10 μM to 800 μM	259 μM	[55]
	Gold Nanoparticles/ Uricase	LSPR	0.0082 nm/μM	10 μM to 800 μM	206 μM	
	polyaniline-zinc oxide/enzyme-Urease	Evanescent wave	n.a	1 M−10 nM	10 nM	[57]
	Zeolitic imidazolate framework8/ Lipase	Evanescent wave	0.9 nm/nM	0-50 nM	0.23 nM	[58]

2.2. Pathogen and Pesticide Detection

Previously, fiber optic sensors were also used to detect pathogens, such as the dengue virus and the HIV pathogen [59]. Pathogens are infectious agents that cause disease in living organisms. Pathogen measurements using fiber optic sensors are label-free, real-time, and accurate. Tapered fibers are an excellent choice for constructing fiber sensors for pathogen detection due to their small size, strong evanescent mode, and high sensitivity. A selective layer that interacts with the intended pathogen can optimize tapered fiber. This selective interaction causes the light propagation characteristics of the sensor to change, and monitoring these changes can help as a tool to detect pathogens.

A tapered fiber integrated with complementary recombinant antibodies was used to detect Dengue II E proteins. When the wavelength shift was investigated, this sensor showed a sensitivity of 5.02 nm/nM and a detection limit nearing 1 pM. It has a response time of 15 min and is necessary due to the continuous spread of dengue fever in many countries [29].

In [60], an S-tapered fiber was used to detect antigens with a sensitivity of 8.33 10^{-5} RIU. The output spectra of this sensor were studied to determine its performance. An immobilized antibody layer on the tapered region was used to achieve this sensitivity. The sensor could detect contaminants and pathogens in real-time. A tapered fiber sensor was also used to detect dangerous pathogens, such as *Salmonella typhimurium*. The pathogen was detected using a single-mode-multimode-single-mode structure. Prior to use, the multimode fiber was tapered. The pathogen's antibodies, anti-*S. Typhimurium* monoclonal antibodies were then immobilized on the tapered region. The sensor had a response time of 20 min and a detection limit of 247 CFU/mL [61]. A reusable immunoglobulin G (IgG) sensor with an ultra-high sensitivity of 13,936 nm/RIU was demonstrated in [62]. The sensor employed an SMF in an MZI configuration. The SMF was spliced with a large core offset fusion splice. The reported sensitivity was obtained within a narrow RI range of 1.3328–1.3398. This sensor has a staphylococcal protein A and goat anti-human IgG immobilized on its narrowest region to detect human IgG in test samples.

Another sensor with ultra-high sensitivity was formed using a tapered single-mode-no core-single-mode fiber coupler sensing element [63]. Pig IgG antibodies were used as an immobilized layer to detect inactivated *Staphylococcus aureus*. This sensor had a wavelength shift of 2.04 nm.

Tapered fibers are also ideal for pesticide detection. Organophosphate pesticide compounds were detected using a non-adiabatic tapered fiber. A bifunctional cross-linker activates the tapered sensor, and the immobilized layer is acetylcholinesterase. This sensor had a sensitivity of 2,100 nm/RIU and a detection limit of 0.24 mM [26].

2.3. Glucose Level Measurement

Glucose level measurements are important for achieving a higher standard of living. Glucometers are the most widely used sensor for glucose testing due to their high sensitivity and quick measurement [64]. The non-invasive glucose monitoring system is a cutting-edge glucose sensing technology.

Qingshan Yang et al. (2019) [65] and Qingshan Yang et al. (2020) [66], in both works, used the same technique of localized surface plasmon resonance. The coated layer on top of the tapered region is the only difference between the two papers. In the first study, the tapered region was coated with gold nanoparticles (AuNPs), whereas the second work added graphene oxide (GO) to the first layer. The sensing region was synthesized and characterized with glucose oxidase (GOx) to ensure that the sensor is highly specific for glucose detection. Overall, when compared to a single material-coated region, the mixed coated tapered region with AuNPs and GO showed a higher sensitivity of 1.06 nm/mM.

Furthermore, polymeric surfaces are also used for glucose biosensing with the immobilization of GOx [67]. In this research, the coated optical fiber's response and sensitivity were measured to be <0.31 μW and 8.7×10^{-3} μWmM^{-1}, respectively. This study reveals that the selectivity of the irradiated fiber coated with pyrrole/poly(vinyl alcohol)-glucose oxidase is highly selective for glucose.

An optical biosensor was developed by Xiaolan Sun et al. (2018) [68] to test the glucose concentration in human serum. Based on the reversible complexation of glucose with a Poly(butyl acrylate) (PBA) film grown on the cone area of a fiber probe, this sensor probe demonstrated good sensitivity (0.1787%/mM) when tested on three human serum samples. In addition, this tapered SMF glucose sensor achieved good reproducibility, stability, and a wide detection window. Table 2 summarizes the tapered optical fiber results in glucose application.

Table 2. Comparison of tapered optical fiber results in glucose application

Sensing Structure	Sensitive Film	Mechanism Used	Sensitivity	Linear Range	Detection Limit	Ref
Tapered based sensor	Gold Nanoparticles	LSPR technique	0.9261 nm/mM	0mM-10mM	322μM	[65]
	pyrrole/poly (vinyl alcohol)-glucose oxidase	Non-linear regression and the Lineweaver-Burk analysis	$(8.7\times10^{-3}$ μWmM^{-1}	0.5mM-20.0 mM	n.a	[67]
	Graphene oxide (GO) and Gold nanoparticles (AuNPs)	LSPR technique	1.06 nm/mM	0 -11 mM	2.26 mM	[66]
	poly (phenylboronic acid) (polyPBA)	Evanescent wave technique	0.1787%/mM	0–60 mM	5mM	[68]

2.4. Protein Detection

Protein is defined as a natural occurrence and extremely complex substance that consists of amino acid residue joined by peptide bonds. Proteins are found in many different organisms and contain various important biological compounds, such as enzymes, hormones, and antibodies. Due to its biocompatibility and versatility to a wide range of assay conditions, such as variable blood [69] and different clotting factors [70], the protein biosensor plays an important role in the discrimination field. Specific protein is an important component of protein biosensing because studying protein interaction is critical for revealing roles in cellular function and useful for understanding daily living activities and pharmaceutical design. A gold layer can be coated on the fabricated tapered sensor structure to improve the detection sensitivity of the protein. M.Mansor et al. (2020) [71] detected avidin using a single-mode tapered fiber biosensor. The sensor probe was avidin selective, which was achieved by immobilizing a layer of biotin on the tapered fiber region. This work demonstrates a high-sensitivity sensor with a sensitivity of 0.40 ±0.14 nm/pM. It also produced smoother spectral output with a high signal-to-noise ratio. Xiaoqi Liu et al. (2020) [60] proposed an S-tapered fiber biosensor for antigen detection. An antibody was immobilized over the tapered region to improve the detection of the antibody and target antigen. In this study, the salinized fiber had a detection limit of approximately 8.33×10^{-5} RIU. The fiber can be used in a modal interferometer for biosensing applications, such as disease diagnosis and biological specificity recognition due to its low cost, real-time detection, and high integration. Dengue virus (DENV) infection and spread have increased significantly over the last decade. Dengue fever is, without a doubt, one of the most serious problems that most of the world is dealing with today. Y.Mustapha Kamil et al. (2017) [29] and Y.Mustapha Kamil et al. (2018) [72] proposed a Dengue E protein detection using tapered optical fiber in their respective papers. The nanostructure layer on the tapered region distinguishes these two papers. [29] improved the sensor by immobilizing DENV E protein on the tapered region surface. In contrast, in work [72], the tapered region was coated with GO to detect Dengue II E protein. The result shows that the graphene-coated biosensor had a higher sensitivity of 12.77 nm/nM.

3. Conclusion

This paper reviews various types of fiber optic sensors and their most recent biosensing applications by focusing on tapered OFS. It aims to help researchers to comprehend fiber optic sensor technology and give a general overview of the challenges encountered when implementing advanced technology in biosensors. As previously stated, OFS have enormous potential for biosensing applications. However, with a few exceptions, we can conclude that despite its maturity and advantages, OFS technology has yet to realize its full potential in the field of biosensors. The low deployment of OFS in biosensing applications, in our opinion, is due to the following factors. First, despite numerous advantages like high sensitivities, ease of manufacturing, a wide variety of configurations, and versatility, tapered optical fibers have a limited number of practical applications. The

majority of the work was completed in tightly regulated laboratories. The second reason is the instruments' dependability and repeatable output. In addition, it should also be noted that in their most basic form, tapered devices are not selectively sensitive and require specific coatings. Furthermore, issues concerning packaging, handling, and mechanical strength must be addressed.

Acknowledgements

The authors would like to thank Universiti Teknikal Malaysia Melaka (UTeM) and the Ministry of Higher Education (MOHE). This research is supported by funding from MOHE via grant no FRGS/1/2020/FKEKK-CETRI/F00425.

References

1. V. Vali, and R. Shorthill, Applied optics, 15(5), p. 1099-1100 (1976).
2. J. Bucaro, H. Dardy, and E. Carome, The Journal of the Acoustical Society of America, 62(5), p. 1302-1304 (1977).
3. B. Culshaw, D. Davies, and S. Kingsley, Electronics Letters, 13(25), p. 760-761 (1977).
4. Wu, Y., et al., Optics & Laser Technology, 92, p. 74-79 (2017).
5. Y. Qian et al., Sensors and Actuators B: Chemical, 260, p. 86-105 (2018).
6. G. Rajan, Optical fiber sensors: Advanced techniques and applications, CRC press (2017).
7. Y. Zhao et al., Biosensors and Bioelectronics, 142, p. 111505 (2019).
8. Y.Koike, T. Ishigure, and E. Nihei, Journal of lightwave technology, 13(7), p. 1475-1489 (1995).
9. X. Bao, and L. Chen, Sensors, 12(7), p. 8601-8639 (2012).
10. S. Korganbayev et al., Optical Fiber Technology, 41, p. 48-55 (2018).
11. L.Grattan, and B. Meggitt, Optical fiber sensor technology: chemical and environmental sensing, Springer Science & Business Media, vol. 4 (1999).
12. J.M.Corres, et al., Optics letters, 40(21), 4867-4870 (2015).
13. T. Azargoshasb, et al., ACS omega,. 5(35), p. 22046-22056 (2020).
14. S. Azad, et al., Optics & Laser Technology, 90, p. 96-101 (2017).
15. I.Del Villar, et al., Journal of lightwave technology, 31(22), p. 3460-3468 (2013).
16. Z. Samavati, et al., Optics & Laser Technology, 123, p. 105896 (2020).
17. H. Zheng, et al., Optics express,. 28(10), p. 15641-15651 (2020).
18. V. Priyamvada, C. Ajina, and P. Radhakrishnan, Optoelectronics Letters, 14(6), p. 465-469 (2018).
19. T. Okazaki, et al., Analytical Letters, 53(13), p. 2160-2169 (2020).
20. S. Devendiran, and D. Sastikumar, Optics & Laser Technology, 89, p. 186-191 (2017).
21. S. Korposh, et al., Sensors, 19(10), p. 2294 (2019).
22. R. Jarzebinska, et al., Measurement Science and Technology, 20(3), p. 034001 (2009).
23. R.,Jarzebinska et al., Analytical Letters, 45(10), p. 1297-1309 (2012).
24. J. Love, et al., IEE Proceedings J (Optoelectronics), 138(5), p. 343-354 (1991).
25. T. Zhou, et al., Optical Fiber Technology, 45, p. 53-57 (2018).
26. M. Arjmand, et al., Sensors and Actuators B: Chemical, 249, p. 523-532 (2017).
27. H. Fu, et al., Sensors and Actuators B: Chemical, 254, p. 239-247 (2018).
28. Y. Liu, et al., Sensors and Actuators B: Chemical, 301, p. 127136 (2019).
29. Y.M. Kamil, et al., Sensors and Actuators B: Chemical, 257, p. 820-828 (2018).
30. V. Ahsani, et al., *Tapered fiber-optic mach-zehnder interferometer for ultra-high sensitivity measurement of refractive index.* Sensors, 19(7), p. 1652 (2019).
31. M.-j.Yin, et al., Coordination Chemistry Reviews, 376, p. 348-392 (2018).
32. V. Mishra, et al., Sensors and Actuators A: Physical, 167(2), p. 279-290 (2011).
33. F. Baldini, et al., Analytical and bioanalytical chemistry, 402(1), p. 109-116 (2012).
34. F. Chiavaioli, et al., Nanophotonics 6, 663–679 (2017).
35. Y. Peng, et al., Small, 14(29), p. 1800524 (2018).
36. T. Guo, et al., Optics & Laser Technology, 78, p. 19-33 (2016).
37. T. Guo, et al., Sensors, 17(12), p. 2732 (2017).
38. Q. Yao, et al., Sensors and Actuators A: Physical, 209, p. 73-77 (2014).
39. F. Wei, et al. 2017 IEEE 25th Optical Fiber Sensors Conference (OFS), 2017.
40. S. Qiao, Journal of Physics: Conference Series, IOP Publishing, 2019.
41. J.K. Sahota, N. Gupta, and D. Dhawan, Optical Engineering, 59(6), p. 060901 (2020).
42. J. Hao, et al., IEEE Conference Proceedings-Lasers and Electro-Optics Society Annual Meeting-LEOS, 2003.
43. W. Li, et al., Photonic Sensors, 11(1), p. 31-44 (2021).
44. P. Chen, X. Shu, and K. Sugden, Optics letters, 42(20), p. 4059-4062 (2017).
45. H.F.Taylor, Fiber Optic Sensors. CRC Press, p. 35-64 (2017).
46. N. Zhao, et al., Sensors, 18(8), p. 2688 (2018).
47. Fan, P., et al., Optics Express, 28(17), p. 25238-25249 (2020).
48. B.H. Lee, et al., Sensors, 12(3), p. 2467-2486 (2012).
49. X. Li, et al., Sensors and Actuators B: Chemical, 269, p. 103-109 (2018).
50. Q. Liu, et al., Optoelectronics Letters, 13(1), p. 25-28 (2017).
51. C.-H. Chen, W.-T. Wu, and J.-N. Wang, Microsystem Technologies, 23(2), p. 429-440 (2017).
52. M. Marazuela, and M. Moreno-Bondi, Analytical and bioanalytical chemistry, 372(5), p. 664-682 (2002).
53. G. Rocchitta, et al., Sensors, 16(6), p. 780 (2016).
54. S.E. Mowbray, and A.M. Amiri, Diagnostics, 9(1), p. 23 (2019).
55. L. Singh, et al., Optical Fiber Technology, 53, p. 102043 (2019).
56. P. Sharma, V. Semwal, and B.D. Gupta, Optical Fiber Technology, 52, p. 101962 (2019).
57. S. Botewad, et al., Frontiers in Materials, 7, p. 184 (2020).
58. L. Lu, et al., IEEE Sensors Journal, 20(23), p. 14173-14180 (2020).
59. H. Bai, et al., Biomacromolecules, 19(6), p. 2117-2122 (2018).
60. X. Liu, Y. Liu, and Z. Wang, Nanotechnology and Precision Engineering, 3(3), p. 162-166 (2020).
61. S. Kaushik, et al., Optical Fiber Technology, 46, p. 95-103 (2018).
62. B.-T.Wang, and Q. Wang, Optics Communications, 426, p. 388-394 (2018).
63. L. Chen, et al., Sensors and Actuators B: Chemical, 320, p. 128283 (2020).
64. J.L. Cano Perez, et al., Biosensors, 11(3), p. 61(2021).
65. Q.,Yang, et al., Plasmonics, p. 1-8 (2019).
66. Q.,Yang, et al., Optik, 208, p. 164536 (2020).
67. S. Idris, et al., Sensors and Actuators B: Chemical, 273, p. 1404-1412 (2018).
68. X. Sun, et al., Optics Communications, 416, p. 32-35 (2018).
69. L. Coelho, et al., 21(8), p. 087005 (2016).
70. M.A. Shuman, and P.W. Majerus, The Journal of clinical investigation, 58(5), p. 1249-1258 (1976).
71. M., Mansor, et al., Optics & Laser Technology, 125, p. 106033 (2020).
72. Y.M. Kamil, et al., IEEE Journal of Selected Topics in Quantum Electronics, 25(1), p. 1-8 (2018).